

Received September 03, 2021; reviewed; accepted December 20, 2021

Kinetics study and reaction mechanism for titanium dissolution from rutile ores and concentrates using sulfuric acid solutions

Mohamed H. Ismael¹, Hesham S. Mohammed¹, Omneya M. El Hussaini¹, Mohamed F. El-Shahat²

¹ Nuclear Materials Authority, P.O. Box 530, El Maadi, Cairo, Egypt

² Ain Shams University, Faculty of Science, Chemistry Department, Cairo, Egypt

Corresponding author: ismael979@yahoo.com (Mohamed H. Ismael)

Abstract:

Recent developments of acid leaching of titanium concentrates and ores have produced renewed industrial and commercial interest. However, the leaching kinetics and mechanism of these concentrates and ores had received little attention. This work, therefore, addresses the leaching kinetics and mechanism of Ti from a rutile concentrate in sulfuric acid solution. The leaching reaction was controlled by diverse parameters like temperature, particle size, acid concentration, liquid/solid (L/S) ratio, and stirring speed. The leaching kinetics was investigated using the Shrinking Core Model in order to determine the optimum criteria which control the reaction. The kinetics analysis showed that the rate of dissolution of Ti increased by increasing reaction temperature, L/S ratio, and stirring speed, while it decreased upon increasing particle size. The kinetics analysis revealed that the dissolution reaction is controlled by the chemical reaction at the rutile particle surface. Applying the Arrhenius relation, the apparent energy of activation E_a for the leaching reaction was calculated to be 23.4kJ/mol. A semi-empirical overall rate equation was introduced to describe the combined effects of the process variables upon the rate of the dissolution reaction: $1 - (1 - x)^{1/3} = k_0 C_{[H_2SO_4]}^{0.803} (dp)^{-0.518} (L/S)^{0.793} (w)^{0.668} e^{(-23400/RT)} t$

Keywords: leaching kinetics and mechanism, titanium, rutile concentrate, leaching design, shrinking core model

1. Introduction

Reaction kinetics, mechanism, and thermodynamics are fundamental knowledge in the fields of science and engineering areas, such as chemical engineering, metallurgy, food processing, biotechnology, and petroleum engineering (Faraji et al., 2020). Kinetics can be discussed as a tool for investigating the rate of chemical reactions and to understand the different effects of a process variables. Kinetics is associated with engineering design and has diverse applications like: estimation of the volume and size of the reacting materials, designing the reactors, optimization, controlling, and scale-up of the process (Gupta, 2003; Levenspiel, 1999; Sohn and Wadsworth, 1979). The kinetics and reaction mechanism of Ti leaching from its bearing minerals, concentrates, ores, and raw materials using acids and alkali is of great industrial and economic importance. The leaching processes of Ti were extensively investigated in many researches, but the leaching kinetics studies and available data are lack. In hydrometallurgical processes, leaching process is carried out either by agitation of a particulate solid in a solution containing the leaching reagents required (Agitation leaching) (Huang et al., 2016; Jabit and Senanayake, 2018; Zhu et al., 2015), or by causing the solution to pass through a porous solid phase that may be a porous rock or a broken material (Heap leaching) (Sachkov et al., 2019). The most important practical criterion to design a leaching process is to exactly understand the chemical reactions taking place and the factors controlling their rates. The kinetics information can

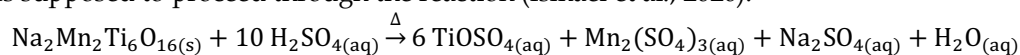
only be derived from experimental and observed data and it is affected by many factors such as: mineralogy, surface area, product layer formation, reactants concentration, particle size, pulp density, agitation, and reaction temperature. The most convenient way to achieve this is to use samples of ground ore or mineral of narrow size range (distribution) for a single substance being studied. For the process control purposes, it is convenient to fit a mathematical model to the relation curve showing dissolution and recovery of the metal values upon leaching as a function of time. The most widely mathematical model used for describing the kinetics of fluid-solid (heterogeneous) chemical reactions of dense particles is the shrinking core model (SCM) (Chen et al., 2013; Houzelot et al., 2018; Niu et al., 2013; Wang et al., 2016). The fluid-solid reactions are several and of great industrial importance.

In this work, the aim was to optimize the kinetics and determine the mechanism of the sulfuric acid dissolution of Ti from rutile concentrates in a manner that may differ from other relevant previous studies. The kinetics data obtained can be used as a guide for other future works, in general, concerning the industrial concept of the sulfuric acid leaching of Ti from ores, rocks, and concentrates.

2. Materials and Methods

2.1. Preface

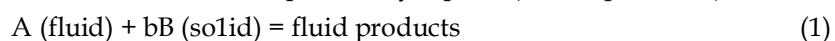
The start Ti-rutile concentrate in this study was prepared by physical upgrading, grinded, alkali roasted, leached with hot water, and the water leach residue (contained Ti) did not dissolve in water. The Ti-rutile concentrate consisted of the oxides of Ti, Fe, Si, Al, V, Mn, and Zr. This Ti-concentrate composed (in wt.%) of 79% TiO₂, 10.05% Fe-oxides, 4.95% MnO, 3.9% SiO₂, 1.5% ZrO₂, 0.9% Al₂O₃, and 0.35% V₂O₅. Upon the roasting process using (NaOH/Na₂CO₃) mixture, these elements' oxides transformed to the corresponding sodium salts of these elements. In the water leaching process, these sodium salts dissolved in water at the beginning of leaching, but, some of these elements re-precipitated again as a solid residue (in situ precipitation) and this conclusion was confirmed in our previous related work (Ismael et al., 2020). The elements completely dissolved in water were Si, Al, and V. The re-precipitated elements were Ti, Zr, Mn, and Fe. We adopted our previous experimental work for the water leaching process to completely attain Ti, Zr, Mn, and Fe in the water leach residue under the optimum leaching conditions, in order to prepare pure V₂O₅ product from the water leach liquor. The crystal structure of the Ti-rutile concentrate and structural transformations occurred in the roasting, water leaching, and sulfuric acid leaching processes were studied using the XRD technique and were illustrated completely in our previous study (Ismael et al., 2020). The water leach residue consisted of well-crystalline and identified forms of (Na₂Mn₂Ti₆O₁₆; ASTM Card No., 052-1308 and Fe₂O₃; ASTM Card No., 79-1741). The Ti dissolution reaction from the water leach residue in sulfuric acid was supposed to proceed through the reaction (Ismael et al., 2020):



The sulfuric acid leaching data reported here, in addition to some data in the previous study, were now analysed using the different models of the SCM to describe the kinetics and mechanism of the dissolution reaction of Ti. The new data in this work comprises studying the effect of particle size (with three different sizes) upon Ti dissolution at different leaching times. The optimum conditions for the sulfuric acid leaching process were determined with respect to Ti dissolution efficiency.

2.2. Kinetics analysis for Ti dissolution and reaction mechanism

A fluid/solid heterogeneous chemical reaction can be expressed by Eqs 1-3 (Levenspiel, 1999):



The dissolution of Ti in sulfuric acid is a typical heterogeneous chemical reaction. So, the dissolution reaction kinetics can be expressed by means of the SCM. The SCM considers that the particle of the solid mass is spherical and the overall reaction rate-controlling process is the slowest step and referred to the most fitting kinetic model. The different kinetic models of the SCM will be

discussed in detail. The leaching data obtained was carefully treated to determine the dissolution reaction kinetics and mechanism.

3. Results and discussion

3.1. Kinetics analysis and reaction mechanism

The kinetics and mechanism for the dissolution reaction of Ti from a rutile concentrate using H₂SO₄ solution were carefully studied using the SCM. Before applying the experimental data to determine the reaction kinetics and mechanism, there are some important concepts and criteria should be declared as will be stated in the following sections.

3.1.1. Overview

It is well evident that the more knowledge about: what the reacting materials are; how they react; and what is occurring during the overall reaction, the more we have to establish a proper design and economic optimization of the process. The most important of these are the reaction kinetics and mechanism.

There are, generally, four fluid-solid reaction kinetics models; the (i) shrinking core, (ii) homogeneous, (iii) pore, and (iv) grain models. The rutile particles, in this study, are essentially compact and close grains, thus could be regarded as non-porous particles. As the rutile particles are rigid and compact but the particle's core gradually shrinks during the leaching process, thus, the most appropriate reaction model should be the shrinking core. The temperature dependence of rutile dissolution can be used to estimate the apparent energy of activation (E_a) and elucidate the kinetics of the process. During the leaching of rutile particles with H₂SO₄ solution, the following main steps may be included: (1) diffusion of the fluid (sulfuric acid) particles through the main body of the fluid film to the particle surface (rutile), this step is turbulence-sensitive; (2) the chemical reaction of the fluid particles with the solid particles at the interface, this step is temperature-sensitive and requires relatively low temperature; (3) the diffusion of both the fluid particles and the products formed through the product ash layer from and back to the fluid body, respectively, this step is temperature-insensitive and requires relatively high temperature, and the activation energy E_a of the chemical reaction step is usually larger than that for mass diffusion (Gupta, 2003; Nie et al., 2020). Also, some of these steps are in series and occur successively, as if any of them is prevented, then the overall reaction will not continue to completion. Recently, some studies and review reports have indicated that the dissolution rate may be controlled by two different successive steps from the previously mentioned steps (Faraji et al., 2020; Li et al., 2010; Tanda et al., 2019; Yang et al., 2014).

The kinetics analysis for a certain chemical reaction is carefully studied to determine the activation energy E_a , and consequently the mechanism, for this reaction. The activation energy is the minimum energy required to cause a reaction to occur. In general, in any reaction mechanism, the rate-determining step is the slowest one, and it determines the overall kinetics of the reaction. In many heterogeneous chemical reactions, as leaching of ores and concentrates, the overall chemical reaction may be the net result of a series of different successive processes which makes the mechanism to be mixed-controlled if more than one step control the reaction rate. This is familiar to reactions occurring at long time periods. The reaction mechanism is the sequence of events that describes the actual process by which reactants become products.

After fitting the experimental data to all the available kinetics models, the best fit model can be determined when it attains some of the following general requirements (Levenspiel, 1999; Li et al., 2010; Sohn and Wadsworth, 1979):

- a. The line of each relation should be straight with relation coefficient (R^2) nearly equals unity.
- b. All the lines should nearly pass the origin, i.e., (have zero-point intercepts).
- c. The film diffusion mechanism can be the rate-controlling step if the homogeneity of the reaction mixture, which is affected with stirring speed (turbulence), is the most effective factor increasing the reaction rate.

- d. The rate-controlling step can be confirmed from experimental data of studying the effect of variation of reaction temperature and particle size upon the reaction rate at different times (only for product diffusion and chemical reaction controls).
- e. The estimated value of E_a , calculated using the Arrhenius relation, may determine the reaction mechanism as it is product diffusion, or chemical reaction, or may be a combination of two different steps. When E_a is $< 20\text{kJ/mol}$ ($\sim 4\text{Kcal/mol}$), the expected mechanism should be product diffusion. If E_a is $> 40\text{kJ/mol}$ ($\sim 10\text{Kcal/mol}$), the expected mechanism should be chemical reaction (Abdel-Aal, 2000; Habashi, 1969; Jackson, 1986).
- f. For the parameter of particle size diameter (r_0), if the rate constant k is directly proportional to the reciprocal of the particle size diameter ($1/r_0$), therefore, the mechanism is expected to occur via chemical reaction control. If the rate constant is directly proportional to the reciprocal of the square of particle size diameter ($1/r_0^2$), therefore, the mechanism is expected to be product diffusion control (Adebayo et al., 2003; Ajemba and Onukwuli, 2012; Baba et al., 2009).

In this study, the kinetics for Ti dissolution reaction from the rutile concentrate in sulfuric acid solution can be described by means of the SCM (Chen et al., 2013; Huang et al., 2016; Jabit and Senanayake, 2018; Niu et al., 2013; Sui and Zhai, 2014; Tanda et al., 2019; Zhu et al., 2015). The reaction process variables studied are: 1) the reaction temperature; 2) the sulfuric acid concentration; 3) the rutile particle size; 4) liquid/solid ratio; and 5) stirring speed. The whole variables were studied at different reaction time intervals.

3.1.2. Effect of reaction temperature

It was found experimentally that for leaching temperatures above 50°C and leaching times more than 30 min Ti began to hydrolyze and reprecipitate in the sulfate leach solutions. So, **Fig. 1** illustrates the effect of leaching temperatures (30, 40, and 50°C) at leaching times (10, 20, and 30 min) to show the increasing Ti dissolution region. The data in Fig. 1 was used to evaluate the kinetics and mechanism for the dissolution reaction of Ti.

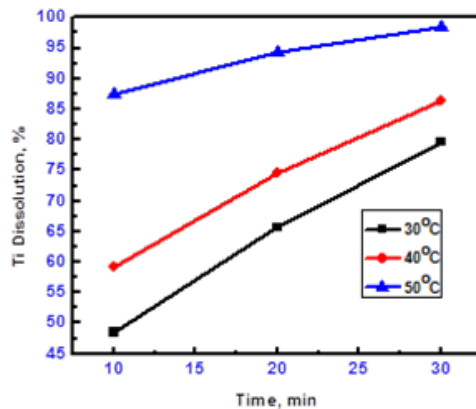


Fig. 1. Effect of leaching temperatures (30, 40, and 50°C) on Ti dissolution at (10, 20, and 30 min) leaching times (Ismael et al., 2020)

The SCM takes several forms that can be effectively applied to determine the reaction rate-controlling step and reaction mechanism for the data in Fig. 1 with its most familiar kinetics models as follows:

3.1.2.1. The surface chemical reaction control

If the leaching process is controlled by the chemical reaction at the surface of the shrinking particle, the following expression of the SCM can be used to describe the leaching kinetics Eq. 4:

$$1 - (1 - x)^{1/3} = Kt \quad (4)$$

where (x) is the fraction of Ti (%) dissolved in sulfuric acid at time t and K is the reaction rate. According to Eq. 4 and the experimental data of Ti leaching rate in **Fig. 1**, the values of $[1 - (1 - x)^{1/3}]$ were calculated and plotted against the reaction time t and the results are shown in Fig. 2a.

3.1.2.2. The diffusion through the product ash layer control

If the leaching process is controlled by the diffusion of reactants and products through the product ash layer formed during the reaction, the following expression of the SCM can be used to describe the leaching kinetics Eq. 5:

$$1 - 3(1 - x)^{\frac{2}{3}} + 2(1 - x) = Kt \quad (5)$$

According to Eq. 5 and experimental data for Ti leaching rate in Fig. 1, the values of $[1 - 3(1 - x)^{\frac{2}{3}} + 2(1 - x)]$ were calculated and plotted against the reaction time t , the results are shown in Fig. 2b.

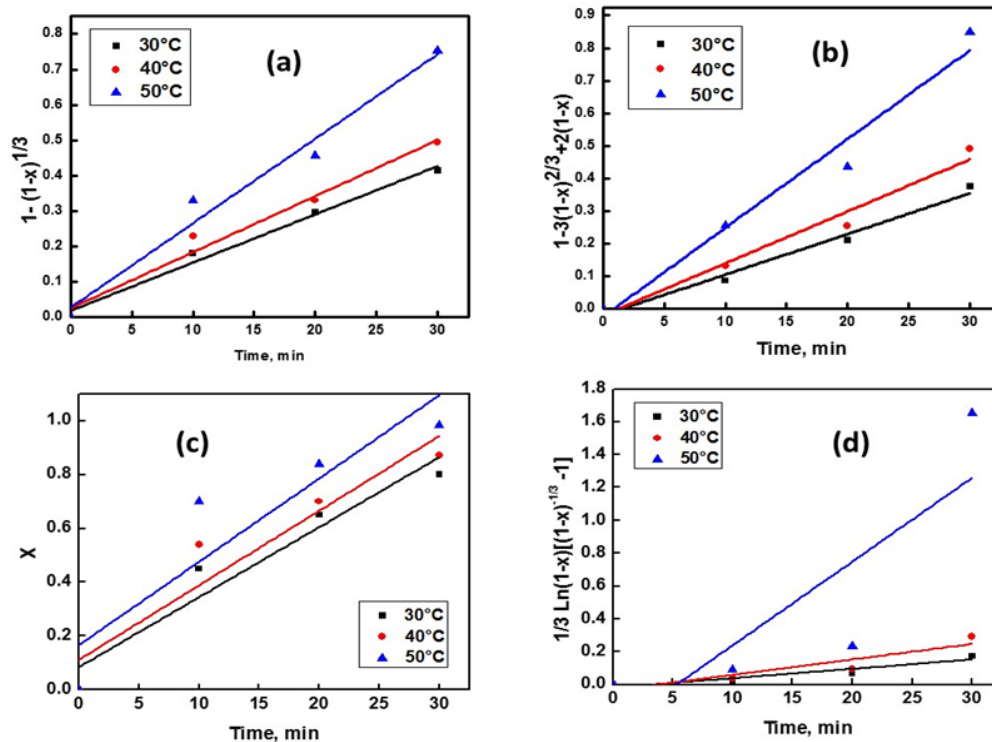


Fig. 2. The SCM kinetic models: (a) chemical reaction, (b) product diffusion, (c) liquid film diffusion, and (d) interface transfer and product diffusion

3.1.2.3. The liquid film diffusion control

This model refers to the diffusion of the fluid molecules through the body film of the fluid to the surface of the solid as described by Eq. 6:

$$X = Kt \quad (6)$$

According to Eq. 6 and the experimental data for Ti leaching rate in Fig. 1, the values of (x) were calculated and plotted against the reaction time t and the results are shown in Fig. 2c.

A new model for the reaction to produce a shrinking core was introduced and developed. It considers the reaction rate to be controlled by two successive (or mixed) operations namely; the interface transfer and the diffusion across the product ash layer (Li et al., 2010; Nie et al., 2020; Tanda et al., 2019; Yang et al., 2014). It can be represented as will be now described.

3.1.2.4. The interface transfer and product diffusion control

This model is expressed by Eq. 7:

$$\frac{1}{3} \ln(1 - x) + [(1 - x)^{-1/3} - 1] = Kt \quad (7)$$

According to Eq. 7 and the experimental data for Ti leaching rate in Fig. 1, the values of $\frac{1}{3} \ln(1 - x) + [(1 - x)^{-1/3} - 1]$ were calculated and plotted against the reaction time t and the results are shown in Fig. 2d.

In the calculations and from all previous data for the various SCM models, the mechanism of the dissolution of Ti using sulfuric acid can be determined from the plots in Fig. 2. It was found that the plots for both the chemical reaction and the product ash diffusion controls are nearly similar with more acceptable values of relation coefficient (R^2) and with nearly zero-point intercepts when compared to the other kinetics models. Thus, and unfortunately, this similarity between the two models made it so difficult to determine whether the dissolution mechanism is either controlled by chemical reaction or product ash diffusion. The (R^2) values for the different kinetic models of the SCM at different temperatures are shown in Table 1.

Table 1. The correlation coefficients (R^2) values for the different kinetic models of the SCM at different temperatures

Leaching temperature, °C	Kinetic expression, R^2			
	$1 - (1 - x)^{1/3}$	$1 - 3(1 - x)^{2/3} + 2(1 - x)$	X	$\frac{1}{3} \ln(1 - x) + [(1 - x)^{-1/3} - 1]$
30	0.9811	0.9713	0.8986	0.8513
40	0.9673	0.9616	0.8525	0.7791
50	0.9626	0.9575	0.7562	0.5721

Though, the dissolution mechanism can be confirmed from the activation energy E_a that is determined from the Arrhenius relation. The relation between the leaching temperature and the rate constant K obtained from Eqs. 4 and 5, for chemical reaction and product diffusion models, can be expressed by the Arrhenius expression Eq. 8 (Houzelot et al., 2018; Levenspiel, 1999):

$$K_r = Ae^{-E_a/RT} \quad (8)$$

where K_r is the overall rate constant, A is the frequency factor, E_a is the apparent activation energy (J/mol), R is the gas constant (8.3144 J/mol.K) and T is the leaching temperature (K). Plotting the values of $\ln K$ obtained from Fig. 2a and Fig. 2b at the corresponding leaching temperatures vs $1/T$ gave straight lines with relation coefficients (R^2) = 0.868 and 0.912, respectively as shown in Fig. 3. Again, the difference between the two values of R^2 is not significant. From the slopes of the two plots, the corresponding values of E_a for the chemical and product diffusion controls were calculated to be 23.4 and 32.5 kJ/mol, respectively. These values, till this point, cannot exactly determine the reaction mechanism.

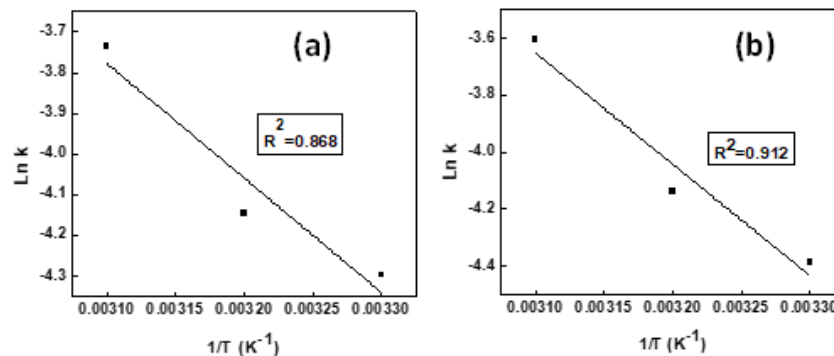


Fig. 3. Arrhenius plots for: (a) chemical reaction, and (b) product diffusion-controlled mechanisms

Although it is reported in literature that if a relatively small change in temperature results in a large increase in the reaction rate, then the reaction is chemically controlled, and thus this step ceases to be rate-controlling at high temperatures. As shown in Fig. 1, the rate of dissolution reaction of Ti from the rutile concentrate increased rapidly from 30 to 50°C which can be considered as a relatively small change in temperature (Gupta, 2003), however, the mechanism in the present study is still unconfirmed till now. In such a complicated case the reaction mechanism, either it is chemical or product diffusion controlled, can be determined and clearly distinguished by studying the effect of variation of particle size upon the rate of Ti dissolution reaction.

3.1.3. Effect of particle size

The effect of particle size was studied in three different fractions: [(-0.250 to +0.125), (-0.125 to +0.075), and (-0.075 to +0.025) mm] at different leaching times (10, 20, and 30 min) as shown in Fig. 4a, and the fixed experimental conditions were: leaching temperature 50°C, [H₂SO₄]=9.2 M, L/S ratio 10 cm³/g, and stirring speed 250 rpm.. It is clear from Fig. 4a that the dissolution rate of Ti is inversely proportional to the particle size and increased with decreasing particle size. The particle diameter (r_0) used in the kinetics calculations for each particle size fraction was chosen to be the average particle size as follows: for the fraction (-0.250 to +0.125) the average is (0.187 mm), for the fraction (-0.125 to +0.075) the average is (0.100 mm), and for the fraction (-0.075 to +0.025) the average is (0.050 mm).

The data in Fig. 4a was applied for both the chemical reaction and product diffusion models according to Eqs. 4 and 5, respectively. The plots for both models are shown in Fig. 4b and Fig. 4c, respectively. Also, the values of (R^2) corresponding to each line for both chemical reaction and product diffusion models are shown in Table 2.

Table 2. Correlation coefficients (R^2) values for the chemical reaction and product diffusion kinetic models at different particle diameters

Particle diameter (r_0), mm	Kinetic expression, R^2	
	$1 - (1 - x)^{1/3}$	$1 - 3(1 - x)^{2/3} + 2(1 - x)$
0.187	0.9986	0.9291
0.100	0.9952	0.9612
0.050	0.9862	0.9653

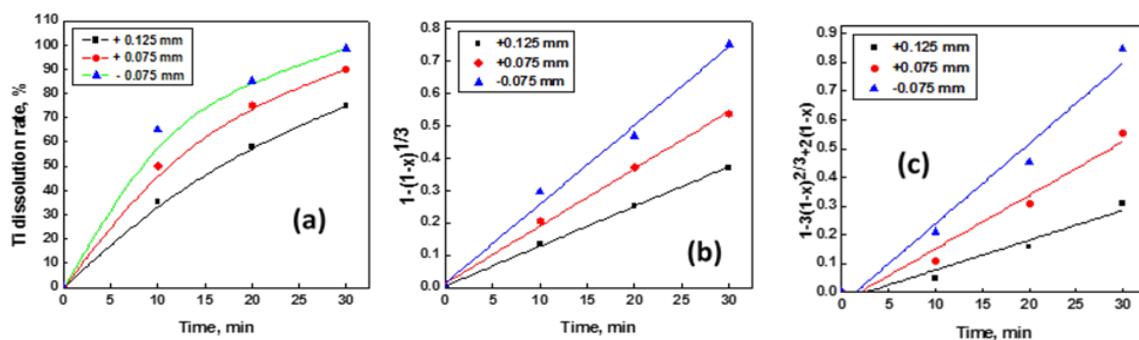


Fig. 4. Variation of (a) Ti dissolution rate, (b) $1 - (1 - x)^{1/3}$, and (c) $1 - 3(1 - x)^{2/3} + 2(1 - x)$, with variation of particle size at different times

From the data in Fig. 4b and Table 2, it is now clear that the chemical reaction mechanism is more acceptable than the product diffusion where the values of (R^2) are greater and the lines nearly pass the origin. Also, the relations between $\ln k$ vs $1/r_0$ (for chemical mechanism) and $\ln k$ vs $1/r_0^2$ (for product diffusion mechanism) are determined and shown in Fig. 5a and Fig. 5b, respectively. It is also clear that the value of (R^2) in Fig. 5a is greater than that in Fig. 5b which supports the chemical reaction mechanism. Referring to Fig. 3a, the calculated E_a for the dissolution reaction of Ti in sulfuric acid solutions from a rutile concentrate is 23.4 kJ/mol, which is in spite of being < 40kJ/mol, but it is still in accordance with a chemical reaction mechanism that was reported in some other publications (Dreisinger and Abed, 2002; Espiari et al., 2006; Jackson, 1986). For the activation energy value that was estimated from the Arrhenius plot, some studies showed that some diffusion-controlled reactions have unusually high activation energy. For instance, the activation energy for the diffusion-controlled dissolution of Ti and Fe from ilmenite in hydrochloric acid solution was reported to be 48.9 and 53.7 kJ/mol, respectively (Tsuchida et al., 1982). Also, Olanipekun 1999 reported the diffusion-controlled dissolution of Ti and Fe from a Nigerian ilmenite ore by hydrochloric acid and calculated the E_a to be 67.1 kJ/mol for Ti and 62.4 kJ/mol for Fe, respectively. Similarly, the E_a for the diffusion-controlled hydrochloric acid leaching of Fe from bauxite varied from 62 to 79 kJ/mol for different particle size fractions (Paspaliaris and Tsolakis 1987). Wang et al., 2013 reported a process to decompose Ti slag by

using the NaOH/KOH binary molten salt. The kinetics investigation indicated that the decomposition of the slag is controlled by mass diffusion in the residual layer and the E_a is 43.1 kJ/mol. On the other hand, other studies showed that some reactions with chemical-controlled mechanism have unusual low activation energies. For example, Nayl et al., 2009 reported the digestion of an ilmenite slag in 4 M NH_4OH solution at a temperature of 150 °C, the slag decomposed with the formation of ammonium titanate which was readily hydrolyzed in hot water to high purity anatase. Analysis of the reaction kinetics found that the reaction was a chemical-controlled process with E_a equaled 27.8 ± 1.6 kJ/mol. On closer examination, it appears that the rate-controlling mechanism of heterogeneous dissolution reactions is sometimes better predicted from plots of the kinetic equations rather than from the activation energy value. In some instances, the same mechanistic information is derivable from both variables (Olanipekun 1999). The reaction mechanism is now confirmed to be controlled by the surface chemical reaction, so, from the slope of Fig. 5a, the reaction order with respect to particle size was found to be (-0.518).

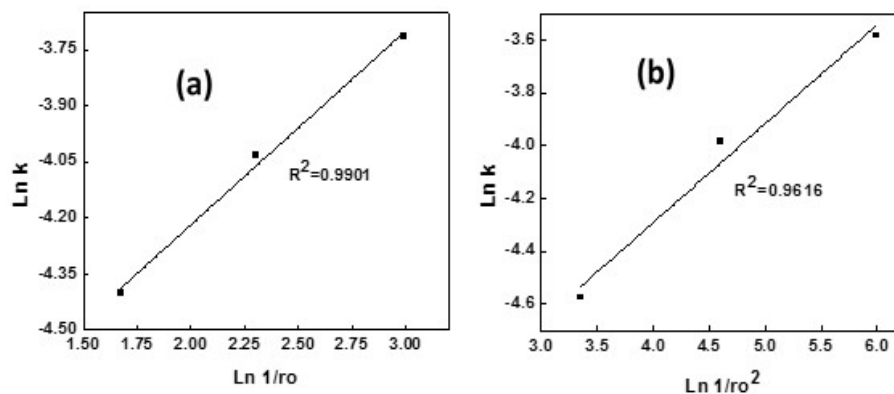


Fig. 5. The relationship between (a) $\ln(k)$ vs $1/r_0$ and (b) $\ln(k)$ vs $1/r_0^2$

3.1.4. Effect of sulfuric acid concentration

The effect of sulfuric acid concentration was studied for different concentrations: (1.8, 2.3, 3.0, 4.6, 6.1, and 9.2 M) at different leaching time intervals. The experimental data obtained were applied to the chemical reaction model and the results are shown in Fig. 6a. A relation between $\ln k$ vs $\ln [\text{H}_2\text{SO}_4]$ was constructed which gave a straight line with a slope equals (0.803) which represents the reaction order with respect to sulfuric acid concentration Fig. 6b.

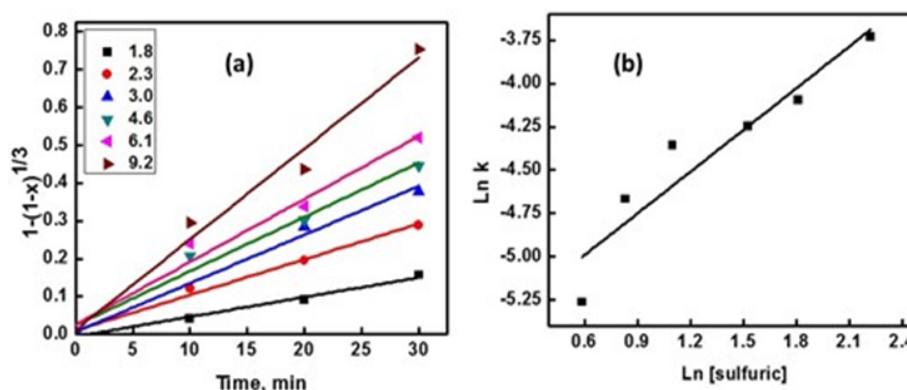


Fig. 6. Variation of (a) $1 - (1-x)^{1/3}$ with variation of $[\text{H}_2\text{SO}_4]$ at different times, and (b) $\ln(k)$ vs $\ln([\text{H}_2\text{SO}_4])$ for chemical reaction control

3.1.5. Effect of liquid/solid (L/S) ratio

The effect of L/S ratio was studied for different ratios: (2, 4, 6, 8, and 10, cm^3/g) at different leaching time intervals. The experimental data obtained were applied to the chemical reaction model and the results are shown in Fig. 7a. A relation between $\ln k$ vs $\ln L/S$ ratio was constructed which gave a

straight line with a slope equals (0.793) which represents the reaction order with respect to L/S ratio as shown in Fig. 7b.

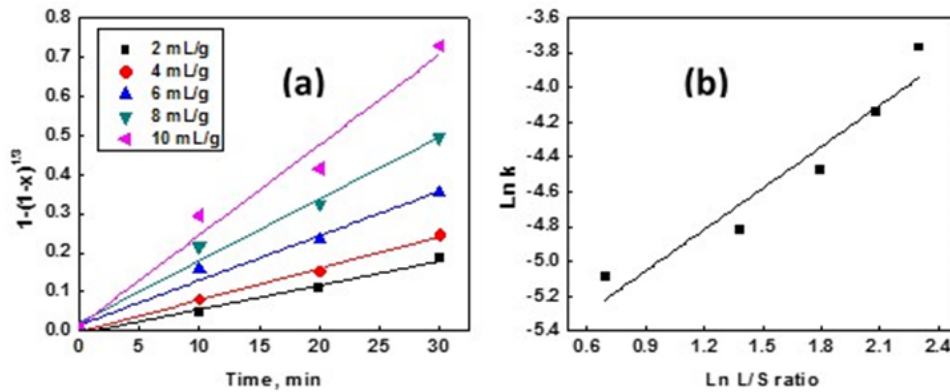


Fig. 7. Variation of (a) $1 - (1 - x)^{1/3}$ with variation of L/S ratio at different times, and (b) $\ln(k)$ vs $\ln(L/S)$ for chemical reaction control

3.1.6. Effect of stirring speed

The effect of stirring speed was studied for different speeds: (150, 250, and 350 rpm) at different leaching time intervals. The experimental data obtained were applied to the chemical reaction model and the results are shown in Fig. 8a.

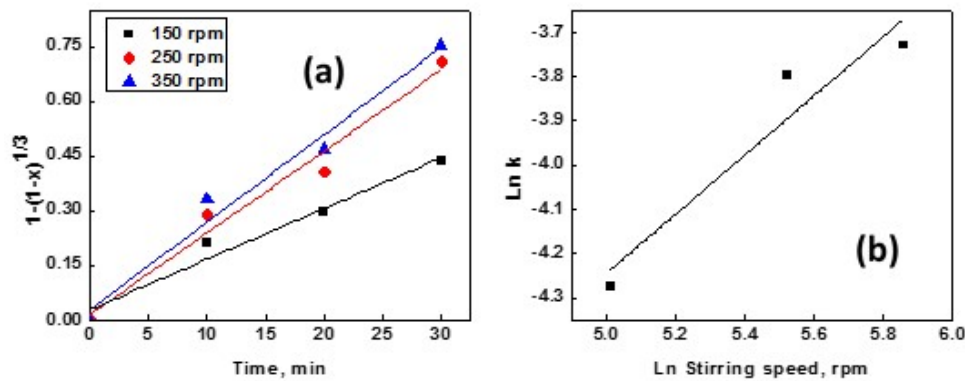


Fig. 8. Variation of (a) $1 - (1 - x)^{1/3}$ with variation of stirring speed at different times, and (b) $\ln(k)$ vs $\ln(\text{stirring speed})$ for chemical reaction control

A relation between $\ln k$ vs \ln stirring speed was constructed which gave a straight line with a slope equals (0.668) which represents the reaction order with respect to stirring speed as shown in Fig. 8b. From all of the previous statistical and graphical calculations, the combined effects of the process variables on the dissolution kinetics of Ti from a rutile concentrate using sulfuric acid can be expressed by the overall rate equation, Eq. 8 (Ajemba and Onukwuli, 2012).

$$1 - (1 - x)^{1/3} = k_0 C_{[\text{H}_2\text{SO}_4]}^a (dp)^b (L/S)^c (w)^d e^{(-E_a/RT)} t \quad (8)$$

where the constants a, b, c, and d are the reaction orders with respect to sulfuric acid concentration, particle diameter, L/S ratio, and stirring speed, respectively. Substituting the values calculated for these constants and the value calculated for activation energy, the semi-empirical overall rate equation becomes as follows, Eq. 9.

$$1 - (1 - x)^{1/3} = k_0 C_{[\text{H}_2\text{SO}_4]}^{0.803} (dp)^{-0.518} (L/S)^{0.793} (w)^{0.668} e^{(-23400/RT)} t \quad (9)$$

4. Conclusions

The leaching kinetics and mechanism of Ti from a rutile concentrate in sulfuric acid solution was carefully investigated. The leaching reaction was affected by temperature, particle size, acid

concentration, liquid/solid ratio, and stirring speed. The leaching kinetics was investigated using the Shrinking Core Model in order to determine the optimum criteria which control the reaction. The kinetics analysis revealed that the dissolution reaction is controlled by the chemical reaction at the rutile particle surface. Applying the Arrhenius relation, the apparent energy of activation E_a for the leaching reaction was calculated to be 23.4kJ/mol. A semi-empirical overall rate equation was introduced to describe the combined effects of the process variables upon the rate of the dissolution reaction.

References

- ABDEL-AAL, E.A., 2000. *Kinetics of sulfuric acid leaching of low-grade zinc silicate ore*. Hydrometallurgy, 55, 247–254.
- ADEBAYO, A.O., IPINMOROTI, K.O., AJAYI, O.O., 2003. *Dissolution Kinetics of Chalcopyrite with Hydrogen Peroxide in Sulphuric acid Medium*. Chem. Biochem. Eng. Q. 17(3) 213–218.
- AJEMBA, R.O., ONUKWULI, O.D., 2012. *Application of the shrinking core model to the analysis of alumina leaching from Ukpor clay using nitric acid*. International Journal of Engineering Research & Technology. Vol. 1 Issue 3.
- BABA, A.A., ADEKOLA, F.A., TOYE, E.E., BALE, R.B., 2009. *Dissolution Kinetics and Leaching of Rutile Ore in Hydrochloric Acid*. Journal of Minerals & Materials Characterization & Engineering, Vol. 8, No.10, 787-801.
- CHEN, D., ZHAO, L., QI, T., HU, G., ZHAO, H., LI, J., WANG, L., 2013. *Desilication from titanium–vanadium slag by alkaline leaching*. Trans. Nonferrous Met. Soc. China 23, 3076–3082.
- DREISINGER, D., ABED, N., 2002. *A fundamental study of the reductive leaching of chalcopyrite using metallic iron Part I: kinetic analysis*. Hydrometallurgy 66(1–3), 37–57.
- ESPIARI, S., RASHCHI, F., SADRNEZHAAD, S.K., 2006. *Hydrometallurgical treatment of tailings with high zinc content*. Hydrometallurgy, 82, 54–62.
- FARAJI, F., ALIZADEH, A., RASHCHI, F., MOSTOUFI, N., 2020. *Kinetics of leaching: a review*. De Gruyter Rev Chem Eng. <https://doi.org/10.1515/revce-2019-0073>
- GUPTA, C.K., 3002. *Chemical Metallurgy: Principles and Practice*. WILEY-VCH Verlag GmbH & Co. KGaA, Weinheim, pp. 336-337.
- HABASHI, F., 1969. *Principles of Extractive Metallurgy*, Vol. 1 Gordon & Breach, New York, pp. 153–163.
- HOUZELOT, V., RANC, B., LAUBIE, B., SIMONNOT, M., 2018. *Agromining of hyperaccumulator biomass: Study of leaching kinetics of extraction of nickel, magnesium, potassium, phosphorus, iron, and manganese from Alyssum murale ashes by sulfuric acid*. Chem Eng Res Des., 129, 1–11.
- HUANG, Y., CHAI, W., HAN, G., WANG, W., YANG, S., LIU, J., 2016. *A perspective of stepwise utilization of Bayer red mud: step two-extracting and recovering Ti from Ti-enriched tailing with acid leaching and precipitate flotation*. J. Hazard. Mater., 307, 318–327.
- ISMAEL, M.H., EL HUSSAINI, O.M., EL-SHAHAT, M.F., 2020. *New method to prepare high purity anatase TiO₂ through alkaline roasting and acid leaching from non-conventional minerals resource*. Hydrometallurgy, 195, 105399.
- JABIT, N.A., SENANAYAKE, G., 2018. *Characterization and Leaching Kinetics of Ilmenite in Hydrochloric Acid solution for Titanium Dioxide Production*. IOP Conf. Series: Journal of Physics: Conf. Series. doi:10.1088/1742-6596/1082/1/012089
- JACKSON, E., 1986. *Hydrometallurgical extraction and reclamation*. Ellis Horwood Ltd, Chichester.
- LEVENSPIEL, O., 1999. *Chemical reaction engineering*. 3rd ed. John Wiley & Sons. New York. 566-588.
- LI, M., WEI, C., QIU, S., ZHOU, X., LI, C., DENG, Z., 2010. *Kinetics of vanadium dissolution from black shale in pressure acid leaching*. Hydrometallurgy 104, 193–200.
- NAYL, A.A., ISMAIL, I.M., ALY, H.F., 2009. *Ammonium hydroxide decomposition of ilmenite slag*. Hydrometallurgy 98, 196–200.
- NIE, W., WEN, S., FENG, Q., LIU, D., ZHOU, Y., 2020. *Mechanism and kinetics study of sulfuric acid leaching of titanium from titanium-bearing electric furnace slag*. J Mater Res Technol., 9(2), 1750-1758.
- NIU, L., ZHAND, T., NI, P., LU, G., OUYANG, K., 2013. *Fluidized-bed chlorination thermodynamics and kinetics of Kenya natural rutile ore*. Trans. Nonferrous Met. Soc. China 23, 34483455.
- OLANIPEKUN, E., 1999. *A kinetic study of the leaching of a Nigerian ilmenite ore by hydrochloric acid*. Hydrometallurgy 53, 1–10.
- PASPALIARIS Y., TSOLAKIS Y., 1987. *Reaction kinetics for the leaching of iron oxides in diasporic bauxite from the Parnassus–Giona Zone Greece by hydrochloric acid*. Hydrometallurgy 19, 259–266.

- SACHKOV, V.I., NEFEDOV, R.A., ORLOV, V.V., 2019. *Column simulation of Fe, Ti, V heap leaching from titanomagnetite ore*. IOP Conf. Ser.: Mater. Sci. Eng. 597 012008. doi:10.1088/1757-899X/597/1/012008
- SOHN, H.Y., WADSWORTH, M.E., 1979. *Rate Processes of Extractive Metallurgy*, Plenum Press, New York. DOI 10.1007/978-1-4684-9117-3
- SUI, L., ZHAI, Y., 2014. *Reaction kinetics of roasting high-titanium slag with concentrated sulfuric acid*. Trans. Nonferrous Met. Soc. China 24, 848–853.
- TANDA, B.C., EKSTEEN, J.J., ORABY, E.A., O'CONNOR, G.M., 2019. *The kinetics of chalcopyrite leaching in alkaline glycine/glycinate solutions*. Minerals Engineering 135, 118-128.
- TSUCHIDA, H., NARITA, E., TAKEUCHI, H., ADACHI, M., OKABE, T., 1982. *Manufacture of high pure titanium (IV) oxide by the chloride process: I. Kinetic study on leaching of ilmenite ore in concentrated hydrochloric acid solution*. Bull. Chem. Soc. Jpn. 55(6), 1934–1938.
- WANG, D., WANG, Z., QI, T., WANG, L., XUE, T.Y., 2016. *Decomposition kinetics of titania slag in eutectic NaOH-NaNO₃ system*. Metall. Mater. Trans. B. DOI: 10.1007/s11663-015-0491-y
- WANG, D., CHU, J., LIU, Y., LI, J., XUE, T., WANG, W., QI, T., 2013. *Novel Process for Titanium Dioxide Production from Titanium Slag: NaOH-KOH Binary Molten Salt Roasting and Water Leaching*. Ind. Eng. Chem. Res., 52, 15756–15762.
- YANG Z., LI H., YIN X., YAN Z., YAN X., XIE B., 2014. *Leaching kinetics of calcification roasted vanadium slag with high CaO content by sulfuric acid*. International Journal of Mineral Processing 133, 105–111.
- ZHU, X., LI, W., GUAN, X., 2015. *Kinetics of titanium leaching with citric acid in sulfuric acid from red mud*. Trans. Nonferrous Met. Soc. China 25, 3139–3145.